A reduced orbital method for large-system electronic structure calculations

1995 J. Phys.: Condens. Matter 7 9219

(http://iopscience.iop.org/0953-8984/7/48/011)

J. Phys.: Condens. Matter 7 (1995) 9219–9233. Printed in the UK

A reduced orbital method for large-system electronic structure calculations

Lin-Wang Wang†§ and Michael P Teter‡

† Laboratory of Atomic and Solid State Physics, Cornell University, USA§

‡ Applied Process Research, Corning Inc., Laboratory of Atomic and Solid State Physics, Cornell University, USA

Received 3 April 1995, in final form 17 July 1995

Abstract. A new method using a small fixed number (much less than the total number of electrons in the system) of orbitals to calculate the electronic structure of an arbitrarily large system is presented. For crystals, this method reduces to a conventional Brillouin zone k-point integration method with the total number of states of all the k-points equal to the number of orbitals used in this method. If one uses a fixed number of orbitals the total computational time is linear in the size of the system. The method is applied to two test systems using a plane wave basis and the results are compared with conventional methods.

1. Introduction

Density functional theory [1] is a widely used tool for studying electronic properties for both solid state systems and large molecules [2, 3]. In the local density approximation [4], all energies can be expressed as explicit functions of the total electron density, with the exception of the kinetic energy. In the Kohn–Sham scheme [4], the kinetic energy is defined as the kinetic energy of N single-electron orbitals for a $2N$ electron system (we discuss unpolarized systems and ignore the spin–orbit coupling). Thus we have

$$E_{tot} = E_k + E_v[\rho] \tag{1}$$

and

$$E_k \equiv -\int \sum_{i=1}^{N} \psi_i(r)\nabla^2\psi_i(r)\,\mathrm{d}^3r \tag{2}$$

$$\rho(r) = 2\sum_{i=1}^{N} |\psi_i(r)|^2 \tag{3}$$

$$\int \psi_i(r)\psi_j^*(r)\,\mathrm{d}^3r = \delta_{i,j} \tag{4}$$

where $E_v[\rho]$ is the potential energy, which includes the electron–ion energy, Hartree energy and exchange correlation energy. They all can be written explicitly as functions of $\rho(r)$, using the local density approximation [4, 5]. E_k is the noninteracting single-particle kinetic energy. Using variational principles to solve the minimum of E_{tot}, one gets the following Kohn–Sham equations:

$$-\tfrac{1}{2}\nabla^2\psi_i(r) + V(r)\psi_i(r) = \epsilon_i\psi_i(r) \tag{5}$$

§ Present address: NREL, Cole Boulevard, 1617 Golden, CO 80401, USA.

0953-8984/95/489219+15$19.50

where $V(\mathbf{r}) = \delta E_v[\rho]/\delta\rho$ is the effective total potential which can be expressed as an explicit functional of $\rho(\mathbf{r})$ and ϵ_i is the eigenvalue of $\psi_i(\mathbf{r})$. There are several numerical ways to solve Kohn–Sham equations (5) [5–7]. One widely used way of solving them for large systems is to minimize E_{tot} iteratively by changing $\psi_i(\mathbf{r})$ while keeping the orthonormal conditions equation (4) satisfied for every iteration step [6, 7]. However, the computation to impose the orthonormal constraint is proportional to N^3, because there are $\frac{1}{2}N(N+1)$ pairs of $\psi_i(\mathbf{r})\psi_j(\mathbf{r})$, and the effort of carrying out the integration $\int \mathrm{d}^3\mathbf{r}$ for each pair is proportional to N. As a result, for N larger than a few hundred, the orthonormal constraint dominates the whole computation, and the computation time scales as N^3.

There are several approaches to making the computational time linear in the size of the system [8–20]. One direct way is to make the kinetic energy E_k an explicit functional of the charge density $\rho(\mathbf{r})$, so that no wavefunction ψ_i is needed in the calculation [10]. One can also apply the inverse iteration method (which was originally developed for the tight-binding calculations) to a real-space numerical grid basis, and thus achieve an *ab initio* and linear-in-N method [11]. Other methods include the Green's function approach [20] and the spectrum approach [19]. One widely used approach, however, is to use the Wannier-like localized orbitals [12–14, 17, 18] or the related localized density matrix [15, 16]. Based on the fact that the Wannier functions are exponentially localized for a system with a band gap [21], the calculation can be linearized by describing a Wannier-like orbital in its finite localized region. Various modifications exist in using this approach, which have generated different 'localized orbital' methods [12, 18]. This localization idea can be restated in the following way: The 'local electronic structure' around one point $\mathbf{r}$ (e.g., the kinetic energy density, the electronic charge density $\rho(\mathbf{r})$) and the density matrix $\rho'(\mathbf{r}', \mathbf{r})$, depend only on the total potential V around that point; the points that are far away affect only the Fermi energy. A direct implementation of this idea is to cut the large system into many small parts, and obtain solutions by solving these small parts independently, then 'patching' them together using a common Fermi energy. This approach was suggested by Yang [9]. One disadvantage of this real space 'divide and conquer' scheme is that not all the points in real space are treated equally. There is no 'divide and conquer' in the localized orbital methods, but still not all the points in real space are treated equally in their formalism. This is represented by the positioning of the localized orbitals which in some sense is artificial. Only when a sufficiently large region is used to describe each localized orbital, will the orbital positioning not affect the final results. (Throughout this paper, we will use the 'divide and conquer' picture to facilitate our discussion. Sometimes, we use this phrase to mean that the treatment of all the real space points is not equal. It is also in this sense that we sometimes refer to the localized orbital methods as 'divide and conquer' methods.)

In this work, we present an alternative to the above real space 'divide and conquer' methods to achieve the linear-in-Nscaling. Instead of 'divide and conquer' in real space, the current method is more like a 'divide and conquer' in k-space (borrowing the terminology from periodic systems). More specifically, instead of using N localized orbitals, we use $n(n \ll N)$ spatially extensive orbitals (to be called reduced orbitals). There is no artificial dividing (or positioning) in real space. Like the above methods, the current method scales linearly with N. Because the use of the order-N methodology in electronic structure calculations is still in its development stage, exploring and analysing new methods is useful. Unlike the localized orbital methods, whose implementation for *ab initio* calculations (i.e. not tight-binding-like calculations) needs special care as regards their basis functions, the current method is explicitly designed for and implemented by plane-wave bases. The current work is based on the previous work of [8] with some new results.

2. Theory: the reduced orbital formalism

2.1. The basic formalism

Although our final goal is to abandon the 'divide and conquer' strategy in real space, it will help us to introduce our method conceptually by starting with the real-space 'divide and conquer' method. The main purpose here is to make a connection between the real-space 'divide and conquer' scheme and the current scheme. This connection will help to determine the relationship between different quantities (e.g., the n and Ω in the following). Let us study a large three-dimensional periodic system. We will cut it in x, y, z directions to get m_x, m_y, m_z parts, respectively. Thus, the large system has been divided into $m = m_x \times m_y \times m_z$ small rectangular systems. For simplicity, let us first assume that the large system is roughly 'uniform' in the size scale of the small systems. In other words, all the small systems can have the same size and each of them contains $2n = 2N/m$ electrons, where $2N$ is the number of electrons in the large system. Now, using the 'divide and conquer' strategy, we solve the Schrödinger equation (5) for each small system. Let M be the index of the small system. We then denote the wavefunctions of the small systems as $\phi_{M,i}(r)$, where i runs from 1 to n. The orthonormal condition of equation (4) has changed to

$$\int \phi_{M,i}(r)\phi^*_{M,j}(r)w(r - R_M)\,\mathrm{d}^3r = \delta_{i,j} \tag{6}$$

where R_M is at the centre of small system M, and $w(r-R_M)$ is a weight function localized in the region of the small system M and will be discussed in detail later. The integration $\int \mathrm{d}^3r$ is over the whole space. (For a *strict* real-space 'divide and conquer' method, w is 1 inside the small rectangular and zero elsewhere. Then $\int \mathrm{d}^3r$ is *effectively* defined inside a small system.)

Now, to change the 'divide and conquer' method to a reduced orbital method, we will 'patch' (or say connect) the ith small wavefunctions $\phi_{M,i}(r)$ of all small systems $\{M\}$ into an extensive orbital $\phi_i(r)$. More specifically, we try to construct a spatially extensive wavefunction $\phi_i(r)$ which equals $\phi_{M,i}(r)$ in the region of small system M (here, i still runs from 1 to n). Then the orthonormal condition of equation (6) becomes

$$\int \phi_i(r)\phi^*_j(r)w(r - R_M)\,\mathrm{d}^3r = \frac{1}{m}\delta_{i,j} \tag{7}$$

for all $M \in \{1, \ldots, m\}$. The factor $1/m$ is a result of normalization of $\phi_i(r)$ over the whole space of the large system. The existence of position R_M in equation (7) indicates the remnant of the 'divide and conquer' strategy. One question is whether there is a weight function w, such that the orthonormal condition equation (7) can be satisfied for an arbitrary position R, without introducing excessive constraints on $\phi_i(r)$. Such weight functions w do exist, the simplest one is

$$w(r) = \frac{1}{m}\sum_{k\in\Omega} \mathrm{e}^{\mathrm{i}k\cdot r} \tag{8}$$

where domain Ω is defined as

$$\Omega = \left\{ i_x \frac{2\pi}{L_x}\hat{x} + i_y \frac{2\pi}{L_y}\hat{y} + i_z \frac{2\pi}{L_z}\hat{z} \right\}$$

and

$$i_x \in -(m_x - 1), \ldots, (m_x - 1)$$

$$\begin{aligned} i_y &\in -(m_y-1),\ldots,(m_y-1) \\ i_z &\in -(m_z-1),\ldots,(m_z-1) \end{aligned} \tag{9}$$

where L_x, L_y, L_z are the x, y, z length of the large system. Unlike conventional weight functions which are positive everywhere, the $w(r)$ defined by equation (8) has some small negative values in some regions. (However, we can use other weight functions, e.g., $w'(r) = ((1/m)\sum_{2k\in\Omega}\exp(\mathrm{i}k\cdot r))^2$ for odd m_x, m_y, m_z, which is positive everywhere, and the subsequent equations (10)–(12) will be the same.) Using the $w(r)$ of equation (8), the orthonormal conditions of equation (7) for all small box M is equivalent to the following orthonormal conditions:

$$\int \phi_i(r)\phi_j^*(r)w_k(r)\,\mathrm{d}^3r = \delta_{i,j}\delta_{k,0} \tag{10}$$

for all $k \in \Omega$ and

$$w_k(r) = \mathrm{e}^{\mathrm{i}k\cdot r} \tag{11}$$

(This $w_k(r)$ should not be confused with $w(r)$ of equation (8)). On the other hand, if $\phi_i(r)$ satisfy equations (10) and (11) for all $k \in \Omega$, then they will satisfy

$$\int \phi_i(r)\phi_j^*(r)w(r-R)\,\mathrm{d}^3r = \frac{1}{m}\delta_{i,j} \tag{12}$$

for arbitrary R. Now, there is no remnant of the real-space 'divide and conquer' strategy. The equations (10) and (12) treat all real-space points R equally.

After the reduced orbital $\phi_i(r)$ and their orthonormal conditions equation (10) are established, we can write down the total energy expression using $\phi_i(r)$:

$$E_{tot} = -m\int\sum_{i=1}^{n}\phi_i^*(r)\nabla^2\phi_i(r)\,\mathrm{d}^3r + E_v[\rho] \tag{13}$$

and

$$\rho(r) = 2m\sum_{i=1}^{n}|\phi_i(r)|^2. \tag{14}$$

The prefactor m in equations(13), (14) indicates that each reduced orbital $\phi_i(r)$ has been 'occupied' with $2m$ electrons.

In the above, the equations (10)–(11), (13)–(14) are introduced from the real-space 'divide and conquer' strategy. Another way to introduce our method is to make equations (10)–(11), (13)–(14) the basic *ansatz* of the current scheme. The $\phi_i(r)$ is defined as the variational solution of equation (13) for the minimum E_{tot} under the orthogonalization constraints of equation (10). Equations (13)–(14) define an energy functional $E_{tot}[\phi_i(r)]$ under the constraints of equation (10). The weight function w does not explicitly appear in equations (13)–(14), but rather it implicitly controls $\phi_i(r)$ through the orthogonalization constraints of equation (12) (or equation (10)). This fact is not related to our definition of w (equation (8)); rather, it can be thought as a basic assumption of the *ansatz*.

2.2. *Modifications*

There is one problem in the above equations (10)–(12) and (14). Summing over $i = j = 1,\ldots,n$ of equations (10), (12), and using equation (14), we have

$$\int \rho(r)w_k(r)\,\mathrm{d}^3r = 2N\delta_{k,0} \tag{15}$$

and

$$\int \rho(\boldsymbol{r})w(\boldsymbol{r}-\boldsymbol{R})\,\mathrm{d}^3\boldsymbol{r} = 2n. \tag{16}$$

This is a result of the assumption we made at the begining of section 2.1. that the large system is roughly 'uniform' in the size scale of the small system, so that each equally volumed small system contains $2n$ electrons (equation (16)). (Here and in the following, we will keep using the phrase of 'small systems' for illustration purposes, although we do not have a 'divide and conquer' any more. The 'small system' can be understood as an alias of $w(\boldsymbol{r}-\boldsymbol{R})$. Thus there is one 'small system' defined for each $\boldsymbol{R}$.) But this assumption (and equations (15)–(16)) is usually not true, especially for systems with different material domains (e.g., with vacuum). There are two ways to correct this problem. In the first way (to be called the fixed-occ method; 'occ' stands for occupation), the volume of each small system will be adjusted so that it will contain $2n$ electrons. This is equivalent to modifying $w_{\boldsymbol{k}}(\boldsymbol{r})$ (hence $w(\boldsymbol{r}) \equiv 1/m\sum_{\boldsymbol{k}\in\Omega} w_{\boldsymbol{k}}(\boldsymbol{r})$) according to the charge density $\rho(\boldsymbol{r})$. In the second way (to be called the fixed-vol method; 'vol' stands for volume), the volume of each small system will be fixed (thus $w_{\boldsymbol{k}}(\boldsymbol{r})$ will be fixed), but the number of electrons within each small systems will be changed. We will introduce these two methods in the following treatment.

In the fixed-occ method, we will redefine $w_{\boldsymbol{k}}(\boldsymbol{r})$ so that equations (15) and (16) can be satisfied. One way to do this is to make a transformation $\boldsymbol{r} \to \boldsymbol{\mu}(\boldsymbol{r})$ and let the Jacobian of this transformation satisfy

$$J(\boldsymbol{r} \to \boldsymbol{\mu}(\boldsymbol{r})) = \frac{1}{\rho_0}\rho(\boldsymbol{r}) \tag{17}$$

where ρ_0 is the average density over the whole system. Then $w_{\boldsymbol{k}}(\boldsymbol{r})$ is redefined as

$$w_{\boldsymbol{k}}(\boldsymbol{r}) = \mathrm{e}^{\mathrm{i}\boldsymbol{k}\cdot\boldsymbol{\mu}(\boldsymbol{r})}. \tag{18}$$

After this, it is easy to show that equation (15) (hence, also equation (16)) is satisfied.

To obtain $\boldsymbol{\mu}(\boldsymbol{r})$ for a given $\rho(\boldsymbol{r})$ is easy. One method, which uses a spring-mesh model, is described in [8]. Another straightforward way is to use the following iterations [8]:

$$\boldsymbol{\mu}_{l+1}(\boldsymbol{r}) = \boldsymbol{\mu}_l(\boldsymbol{r}) + \Delta\boldsymbol{\mu}_l(\boldsymbol{\mu}_l(\boldsymbol{r})) \tag{19}$$

and

$$\Delta\boldsymbol{\mu}_l(\boldsymbol{k}) = \begin{cases} \dfrac{\boldsymbol{k}}{k^2}\dfrac{\rho_l(\boldsymbol{k})}{\rho_0} & \text{for } \boldsymbol{k} \neq 0 \\ 0 & \text{for } \boldsymbol{k} = 0 \end{cases} \tag{20}$$

where l is the iteration index, $\boldsymbol{k}$ is the reciprocal vector of the large system and $\rho_l(\boldsymbol{k})$, $\Delta\boldsymbol{\mu}_l(\boldsymbol{k})$ are defined as

$$\rho_l(\boldsymbol{k}) = \int \rho_l(\boldsymbol{\mu}_l)\mathrm{e}^{\mathrm{i}\boldsymbol{k}\cdot\boldsymbol{\mu}_l}\,\mathrm{d}^3\boldsymbol{\mu}_l \tag{21}$$

$$\Delta\boldsymbol{\mu}_l(\boldsymbol{k}) = \int \Delta\boldsymbol{\mu}_l(\boldsymbol{\mu}_l)\mathrm{e}^{\mathrm{i}\boldsymbol{k}\cdot\boldsymbol{\mu}_l}\,\mathrm{d}^3\boldsymbol{\mu}_l \tag{22}$$

where

$$\rho_l(\boldsymbol{\mu}_l) = \rho_{l-1}(\boldsymbol{\mu}_l)/J(\boldsymbol{\mu}_{l-1} \to \boldsymbol{\mu}_l) \tag{23}$$

The iteration starts with $\boldsymbol{\mu}_1 = \boldsymbol{r}$ and $\rho_1(\boldsymbol{\mu}_1) = \rho(\boldsymbol{r})$. The iteration stops when $\rho_l(\boldsymbol{k}) = 0$ for $\boldsymbol{k} \neq 0$. Because, for each iteration, $J(\boldsymbol{\mu}_{l-1} \to \boldsymbol{\mu}_l)$ equals $\rho_{l-1}(\boldsymbol{\mu}_l)$ in the first order of

$\rho_{l-1}(k \neq 0)$, the iteration converges very fast (about 2 to 3 iterations are enough to get a satisfactory $\mu(r)$). Thus calculating $\mu(r)$ from a given $\rho(r)$ is not a problem in practice.

In the fixed-vol method, instead of changing $w_k(r)$, we will change the occupation number in each small system. Assume that we have obtained solution for n orbitals $\phi_i(r)$ with n slightly larger than N/m using orthonormal conditions of equations (10) and (11). Then instead of using equation (14) to get the charge density $\rho(r)$, we will use a new method to obtain it. We first diagonalize the following matrix defined as a function of position R:

$$H_{i,j}(R) = \int w(r-R)\tfrac{1}{2}[\phi_i^*(r)(\hat{H}\phi_j(r)) + \phi_j(r)(\hat{H}\phi_i(r))^*]\,\mathrm{d}^3r \qquad (24)$$

where $w(r-R)$ is defined in equation (8) and $\hat{H} = -\frac{1}{2}\nabla^2 + V(r)$. Let $E_l(r)$ and $u_l(i, R)$ be the eigenvalue and eigenvector of $H_{i,j}(R)$ respectively. Then we can define

$$\phi'_{R,l}(r) = \sum_{i=1}^{n} u_l(i, R)\phi_i(r) \qquad (25)$$

as the lth local eigenfunction at R. Then we can calculate the charge density as

$$\rho(r) = 2m\sum_{R}\sum_{l=1}^{n} F[(E_f - E_l(R))\beta]f(r-R)|\phi'_{r,l}(r)|^2 \qquad (26)$$

where $F(x) = 1/(\mathrm{e}^x + 1)$ is the Fermi occupation function, and $1/\beta$ is a fictitious temperature. $\sum_R$ stands for a summation over a set of points (which includes many more points than m). $f(r-R)$ is a partition function, which satisfies

$$\sum_R f(r-R) = 1 \qquad \text{for all } r. \qquad (27)$$

E_f is a Fermi energy which is determined by requiring the total charge to be $2N$. Finally, the band structure energy of the system (defined as the sum of the occupied eigenvalues of equation (5)) is

$$E_{band} = 2m\int\sum_{R}\sum_{l=1}^{n} F[(E_f - E_l(R))\beta]E_l(R)f(r-R)|\phi'_{R,l}(r)|^2\,\mathrm{d}^3r. \qquad (28)$$

The remaining part of the energy can be calculated as a function of $\rho(r)$. One disadvantage of this method is that we reintroduced the real-space positioning of R, which is reminiscent of the real-space 'divide and conquer' method. However, since the diagonalization of $H_{i,j}(R)$ is fast, we can calculate many R points (far more than m), and we found in practice that the result is insensitive to the positions of R as long as there are more R points than m and $f(r-R)$ is more localized than $w(r-R)$. We also found that the results are insensitive to β as long as it is sufficiently large.

2.3. *The calculation of the reduced orbitals*

In the following, we will discuss the numerical methods to calculate $\phi_i(r)$. The procedures for the fixed-occ and fixed-vol methods are the same, except as regards the definition of $w_k(r)$. Thus they will be treated in the same formalism. The goal is to solve for $\phi_i(r)$ by variationally minimizing E_{tot} of equation (13) while satisfying the orthonormal condition of equation (10) (where $w_k(r)$ is defined by equations (18) and (11) for the fixed-occ and fixed-vol methods respectively). In the fixed-occ method, the charge density $\rho(r)$ should be calculated in each iteration step using equation (14), and $\rho(r)$ will enter the orthogonalization constraint equations of $\phi_i(r)$. In the fixed-vol method, the charge density $\rho(r)$ does not enter the orthogonalization constaint equations of $\phi_i(r)$, and it will only be calculated (using equation (26)) after all the $\phi_i(r)$ have converged. To impose the orthogonalization constraint from equation (10), we add a Lagrangian term from equation (10) to equation (13); then taking a derivative of equation (13) with respect to $\phi_i(r)$, we get the following equation

$$-\tfrac{1}{2}\nabla^2\phi_i(r) + V(r)\phi_i(r) = \sum_{j=1}^{n}\sum_{k\in\Omega} D(i, j, k)w_k(r)\phi_j(r) \tag{29}$$

where $D(i, j, k)$ is a Lagrangian multiplier, and must satisfy the following symmetry condition

$$D(i, j, k) = D^*(j, i, -k) \tag{30}$$

in order to get the true minimum of equation (13). Equation (29) is an analogue of the Schrödinger equation (5) for the Kohn–Sham wave function $\psi_i(r)$. In deriving equation (29), we have ignored the derivative of $w_k(r)$ respect to $\phi_i(r)$ for the fixed-occ method. Thus for the fixed-occ method, strictly speaking, $\phi_i(r)$ is not the exact minimum solution of E_{tot} of equation (13) on the manifold of equation (10). In this case, $\phi_i(r)$ should be considered as the solution of equation (29) while satisfying equation (10). Equations (29) and (10) are the equations we will use to obtain $\phi_i(r)$.

Solving for $\phi_i(r)$ from equation (29) can be done using the conjugate gradient method. The details of using the conjugate gradient method in solving the Schrödinger equation can be found in [22]. (Instead of performing several conjugate gradient steps for each orbital $\phi_i(r)$ separately, in the current method we need to update all the orbitals $\{\phi_i(r)\}$ at the same time within each conjugate gradient step). Here the only difference from the conventional conjugate gradient method is that at each conjugate gradient step, instead of imposing the orthonormal condition of equation (4) we will impose the orthonormal condition of equation (10). We will discuss this in more detail.

Suppose we have a set of wavefunctions $\{p_i(r)\}$, and we want to make them orthogonal to $\{\phi_i(r)\}$ as in equation (10). (The formalism is very similar for other situations, e.g., to make a non-orthonormal set of $\{\phi_i(r)\}$ satisfy equation (10).) We can achieve this by subtracting $\{w_k(r)\phi_i(r)\}$ components from $\{p_i(r)\}$:

$$p_i'(r) = p_i(r) - \sum_{j=1}^{n}\sum_{k\in\Omega} D'(i, j, k)w_k(r)\phi_j(r) \tag{31}$$

and requiring that the resulting $\{p_i'(r)\}$ satisfy

$$\int p_i'(r)^*\phi_j(r)w_k(r)\,\mathrm{d}^3r = 0. \tag{32}$$

On substituting equation (31) into equation (32), we have the following linear equation for a symmetric (satisfying equation (30)) $D'(i, j, k)$:

$$\sum_{i_3=1}^{n}\sum_{k_1\in\Omega}[C(i_1, i_3, k - k_1)D'(i_3, i_2, k_1) + D'(i_1, i_3, k_1)C(i_3, i_2, k - k_1)] = B(i_1, i_2, k) \tag{33}$$

where

$$B(i, j, k) = \int w_{-k}(r)[\phi_j^*(r)p_i(r) + \phi_i(r)p_j^*(r)]\,\mathrm{d}^3r \tag{34}$$

and

$$C(i,j,k)=\int \phi_i(r)\phi_j^*(r)w_{-k}(r)\,\mathrm{d}^3r \tag{35}$$

The k in $C(i,j,k)$ is within domain Ω_2, which is defined as

$$\Omega_2=\left\{i_x\frac{2\pi}{L_x}\hat{x}+i_y\frac{2\pi}{L_y}\hat{y}+i_z\frac{2\pi}{L_z}\hat{z}\right\}$$

and

$$\begin{aligned}
&i_x\in -2(m_x-1),\ldots,2(m_x-1)\\
&i_y\in -2(m_y-1),\ldots,2(m_y-1)\\
&i_z\in -2(m_z-1),\ldots,2(m_z-1).
\end{aligned} \tag{36}$$

Thus, it is twice the size of Ω in each of the x, y, z directions. This is why $C(i,j,k)$ (equation (35), in domain Ω_2) does not equal $\delta_{i,j}\delta_{k,0}$ (equation (10), in domain Ω), because k could be outside the region of Ω.

Now, we will discuss how to calculate $B(i,j,k)$ and $C(i,j,k)$ and how to solve for $D'(i,j,k)$ from equation (33). $C(i,j,k)$ and $B(i,j,k)$ both have the following form:

$$C'(i,j,k)=\int f_{i,j}(r)w_k(r)\,\mathrm{d}^3r \tag{37}$$

The direct calculation of equation (37) could lead to a N^2 scaling. This is because there are n^2 $\{i,j\}$ pair, 4^3m k-points in Ω_2, and each integration of $\int d^3r$ takes $N_{grid}\equiv\alpha N$ operations. Thus the total number of operations for equation (37) is $4^3n^2mN_{grid}=\alpha4^3nN^2$. This is unacceptable for our linear scaling scheme. However, $w_k(r)$ is defined as equation (11) for the fixed-vol method, and equation (18) for the fixed-occ method. Let us first discuss the fixed-vol method. Substituting equation (11) into equation (37), we find that the transformation from r-space into k-space is a Fourier transformation; thus, the fast Fourier transform (FFT) technique can be used. As a result, the total number of operations can be reduced to $\alpha n^2N\log_2(4^3m)$, which is roughly linear in N. After $D'(i,j,k)$ is obtained, the $\sum_{k\in\Omega}D'(i,j,k)w_k(r)$ in equation (31) can be carried out in a similar way using FFT. For the fixed-occ method, $w_k(r)$ is defined in equation (18). To use the same FFT technique, we need to interpolate $\phi_i(r)$ on the uniform r-grid to $\phi_i(\mu(r))$ on a uniform μ-grid (also called a variable μ-grid). Also note that

$$\mathrm{d}^3r=\frac{1}{J}\,\mathrm{d}^3\mu=\frac{\rho_0}{\rho(\mu)}\,\mathrm{d}^3\mu.$$

After these steps, the FFT can be used on the variable μ-grid. The operation for the interpolation is proportional to nN_{grid}, and thus has a linear-in-N scaling.

After $B(i,j,k)$ and $C(i,j,k)$ are obtained, we need to solve for $D'(i,j,k)$ from equation (33). Equation (33) is a linear equation with dimension $2^3mn^2\times2^3mn^2$. Solving it directly using a standard numerical routine is costly and leads to high order scaling in N. However, equation (33) is a sparse linear equation. We have not found a direct method which can utilize its sparseness yet. So, here, we use an iterative method. It is easy to show that $C(i,j,k)$ defines a Hermitian and positive definite matrix in equation (33). As a result, the conjugate gradient method is a proper iterative method for solving the linear equation. The main operation in the conjugate gradient method for solving equation (33) is carrying out the operation of the left-hand side of equation (33). Each $\sum_{k_1\in\Omega}$ is a convolution, and thus can be carried out in $4^3m\log_2(4^3m)$ operations using a standard numerical routine. Thus the whole operation count of the left-hand side of equation (33) is

$4^3mn^3\log_2(4^3m) = 4^3n^2N\ln(4^3m)$ which is roughly linear in N. This conjugate gradient iteration for $D'(i,j,\boldsymbol{k})$ is nested inside the outer iteration for $\{\phi_i(\boldsymbol{r})\}$. We found that using ~ 30 iterations to solve for $D'(i,j,\boldsymbol{k})$ for each outer iteration of $\{\phi_i(\boldsymbol{r})\}$ works well. In plane-wave calculations for large Si systems, we found that the time spent on solving $D'(i,j,\boldsymbol{k})$ using this method, is about half of the total computational time.

Finally, let us mention that, for the fixed-vol method, after equation (29) is solved, $H_{i,j}(\boldsymbol{r})$ of equation (24) can be expressed as

$$H_{i,j}(\boldsymbol{R}) = \sum_{\boldsymbol{k}\in\Omega} B'(j,i,\boldsymbol{k})\mathrm{e}^{\mathrm{i}\boldsymbol{R}\cdot\boldsymbol{k}} \tag{38}$$

where

$$B'(i,j,\boldsymbol{k}) = \tfrac{1}{2}\int w_{-\boldsymbol{k}}(\boldsymbol{r})[\phi_i^*(\boldsymbol{r})(\hat{H}\phi_j(\boldsymbol{r})) + \phi_j(\boldsymbol{r})(\hat{H}\phi_i(\boldsymbol{r}))^*]\,\mathrm{d}^3\boldsymbol{r}. \tag{39}$$

This $B'(i,j,\boldsymbol{k})$ is calculated in the conjugate gradient steps of $\phi_i(\boldsymbol{r})$, so it is readily available. Thus it is fast and straightforward to calculate $H_{i,j}(\boldsymbol{R})$ for many values of $\boldsymbol{R}$.

3. Applications

We now apply the method discussed in the previous section to some testing systems. To simplify the matter, we will treat the system nonselfconsistently. That means that we will use a fixed potential $V(\boldsymbol{r})$ in equations (5) and (29). For selfconsistent calculations, the density errors will only be reduced compared to the current nonselfconsistent results [8]. This is because the Coulomb interaction will ensure a rough local charge neutrality, which will prevent large density errors. The numerical iteration is also stable for selfconsistent calculations [8]. The test for the current approach is to compare the results of equation (29) with the result of equation (5), which will be called 'exact' for the current purpose. The main quantities to be compared are the charge density, the kinetic energy and the potential energy, which are used in total energy calculations.

We will first test a one-dimensional system. Although the above formalism is for three dimensions, it is straightforward to change it to one suitable for one dimension. The system we test is a one-dimensional disorder system consisting of many potential wells, with large fluctuations in both well depth and position. There is also an area of vacuum, so the system is highly nonuniform. The potential of this system is shown in figure 1(a). There are 16 wells in the system. With each well occupied by two electrons, there are 32 electrons (16 orbitals) in the system. Despite the randomness, there is a band gap above the 16 occupied states. The system is first calculated using the full Kohn–Sham equation (5).

In the fixed-occ method, the 16 orbitals have been reduced to 8 orbitals (i.e. $m = 2$, $n = 8$). The calculation for the variable grid $\mu(x)$ in this one-dimensional system is very simple; it is

$$\mu(x) = \frac{L}{Q}\int_0^x \rho(y)\,\mathrm{d}y \tag{40}$$

where L is the length of the system and Q is the total charge. The computations are carried out using a plane-wave basis and the conjugate gradient method as described in section 2.3. The charge density results of this fixed-occ method are shown in figure 1(b) as dots, while the result of equation (5) is shown as the full curve. The difference between these two charge densities is very small. More quantitatively, this difference is calculated as

$$\Delta\rho = \frac{1}{Q}\int |\rho_{exact}(\boldsymbol{r}) - \rho_{approx}(\boldsymbol{r})|\,\mathrm{d}^3\boldsymbol{r}. \tag{41}$$

This difference is 2.6% and is reported in table 1. Also reported in table 1 is the potential, kinetic and total energies of the exact results and the current results. The difference between the fixed-occ method and the exact method is about 1% for these energies.

Table 1. Total, potential and kinetic energies and the charge density errors of the one-dimensional disordered system. The energies are in atomic units.

Methods	E_{tot}	E_v	E_k	$\Delta\rho$
Exact (equation (5))	−4.939	−6.355	1.416	—
Fixed-occ	−4.934	−6.334	1.400	2.6%
Fixed-vol	*−4.889*	*−6.307*	*1.418*	*3.0%*

In the fixed-vol method, 13 orbitals ($n = 13$) are calculated using $m = 2$. (Note: should the system be larger, this number of 13 would not change.) The fictitious temperature $1/\beta$, the positions of $\boldsymbol{R}$ and the size of the partition function $f(\boldsymbol{r} - \boldsymbol{R})$ in equations (26) and (28) do not affect the result in any significant way. The charge density of this method is shown in figure 1(c) and the potential, kinetic and total energies are listed in table 1. The charge density has an error of 3.0% and the energies have a typical error of 1%.

In summary, both the fixed-occ and fixed-vol method work well for this one-dimensional system despite the fact that it is highly nonuniform.

Next, we apply our methods to a real three-dimensional system. The system we choose is Si in a diamond structure with 64-atoms in a supercell. The atoms are randomly moved from their ideal diamond structure positions by $\sim$ 15% of the Si–Si bond length. Thus it is a case where a large supercell calculation is needed. To get the total potential $V(\boldsymbol{r})$, we first performed a selfconsistent calculation. A local pseudopotential is used for the Si atom, although there should be no difficulty in using nonlocal pseudopotentials in the current methods. Despite the large distortion of the diamond structure, the system still has a small band gap. After $V(\boldsymbol{r})$ is obtained, it is fixed in the following calculations. A relatively gross real-space grid of $24 \times 24 \times 24$ is used in a plane-wave-basis calculation. The plane-wave-basis energy cut-off is 8 Ryd. This is relatively small; thus the result is not fully converged with respect to the plane-wave basis. However, this should not affect our comparison between different methods, because they all use the same energy cut-off and real-space grids. First, a full wavefunction calculation using equation (5) and the fixed potential $V(\boldsymbol{r})$ is carried out. There are 128 occupied eigenstates. The charge density is shown in figure 2(a) and energies in table 2.

Table 2. Total, potential and kinetic energies and the charge density errors of the 64-Si-atom system. The potential energy is the nonselfconsistent potential energy, which is the product of the charge density and the potential $V(\boldsymbol{r})$. The energies are the energy per atom in eV.

Methods	E_{tot}	E_v	E_k	$\Delta\rho$
Exact (equation (5))	−33.08	−56.26	23.18	—
Fixed-occ	−33.77	−55.72	21.95	6.9%
Fixed-vol	−32.79	−56.09	23.31	4.5%

Now, in the reduced orbital method, we used $m_x = m_y = m_z = 2$. Thus in the fixed-occ method, the 128 orbitals have been reduced to 16 orbitals ($n = 16$). In the fixed-vol method, we used $n = 19$. To generate the variable grid $\mu(\boldsymbol{r})$ for the fixed-occ method, we have used a $\rho_{ave}(\boldsymbol{r})$ instead of $\rho(\boldsymbol{r})$ in equation (17). Here, $\rho_{ave}(\boldsymbol{r})$ is a locally averaged

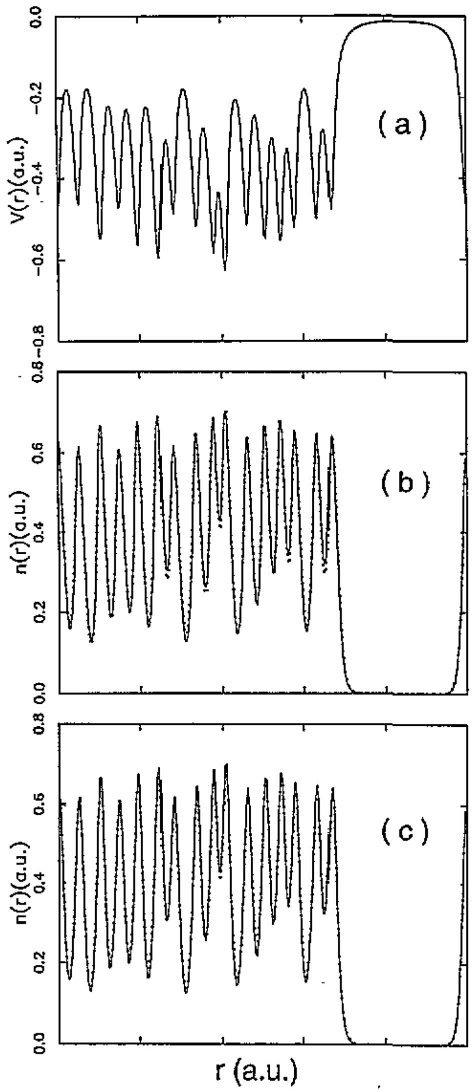

Figure 1. The potential and charge densities of the one-dimensional disordered system: (a) the potential, with a vacuum space at the right-hand side; (b) charge density comparison: the fixed-occ method result (dots) and the exact result (equation (5)) (solid line); (c) charge density comparison: the fixed-vol method result (dots) and the exact result (equation (5)) (solid line).

result of $\rho(r)$. As long as this local average is performed in an area smaller than the area of

$$w(r) \equiv \frac{1}{m} \sum_{k \in \Omega} w_k(r)$$

the use of $\rho_{ave}(r)$ in equation (17) should not affect our final results very much. A spring-mesh model [8] is used to calculate $\mu(r)$ based on $\rho_{ave}(r)$, although similar results can be obtained using equations (19)–(23). The algorithm of using interpolation (for the fixed-occ method) and FFT to calculate $C(i, j, k)$ and $B(i, j, k)$ in equations (31), (34) and (35) is implemented in our computer code, as is the use of conjugate gradient and convolution

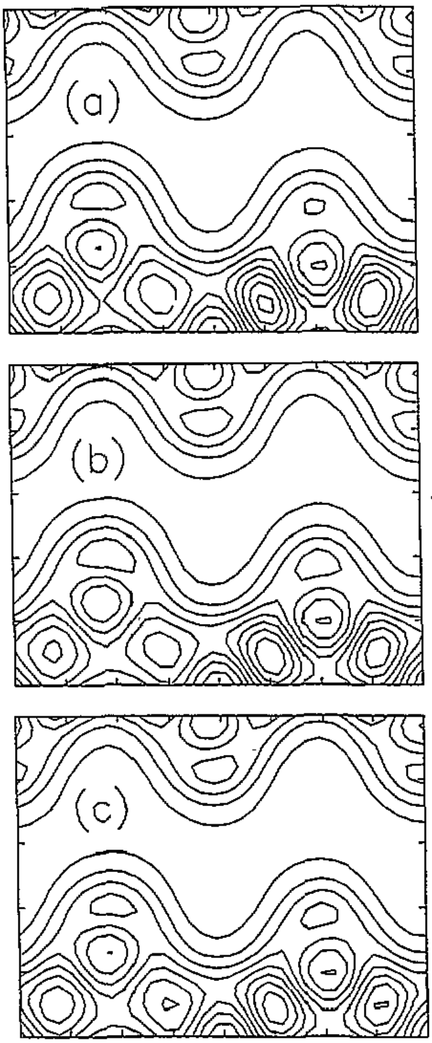

Figure 2. The charge density comparison between different methods for the 64-Si-atom system: (a) the exact method (equation (5)); (b) the fixed-occ method; (c) the fixed-vol method. All contour plots are plotted using the same contour interval of 0.01 au and only one fourth of the [110] cross section of the whole system is shown.

techniques in solving the linear equation (33). Thus the whole computational time scales linearly with the size of the system. Again, in the fixed-vol method, the fictitious temperature $1/\beta$, the positions of $\boldsymbol{R}$ and the size of the partition function $f(\boldsymbol{r}-\boldsymbol{R})$ in equations (26) and (28) have very small effects on the final results. Finally, the charge densities of the fixed-occ and fixed-vol methods are shown in figures 2(b) and 2(c), respectively. The charge density errors calculated according to equation (41) are 6.9% and 4.5% for the fixed-occ and fixed-vol methods, respectively, and are listed in table 2. Also listed in table 2 are their potential, kinetic and total energies. For the fixed-occ method, the largest energy error is in the kinetic energy which is about 5%. For the fixed-vol method, the energy errors are all less than 1%. Overall, the fixed-vol method has better results than the fixed-occ method, in this three-dimensional system. Note that, in the one -dimensional case, the fixed-occ method has similar quality (or even slightly better) than the fixed-vol method; the inferiority of the fixed-occ method in our three-dimensional system might have something to do with the gross real-space grid we used. Because the numerical grid interval is large, the Jacobian in equation (17) is not well defined on the numerical grid, which can introduce an error in the variable grid $\mu(r)$. Also, due to the interpolation scheme we used in the fixed-occ method, there are more chances for numerical inaccuracy in the fixed-occ method.

In summary, the reduced orbital methods work well for the three-dimensional system. With the current implementation of the methods, the computational time scales linearly with the size of the system.

4. Discussion

In the abstract, we mentioned that the reduced orbital method reduces to a k-point integration method in the cases of crystals. If the m small systems (in the discussion of section 2.1) cut from a large system (supercell) are identical, then the n $\bar{\Gamma}$-point Bloch wavefunctions of the small systems satisfy the orthonormal condition equation (10) and the wavefunction equation (29). This is still true when the variable grid μ is used for $w_k(r)$. Because the $\bar{\Gamma}$ point of the small system could correspond to a few k-points in the Brillouin zone of the primary cell (depending on how large the small system (n) is), the current method is equivalent to using these few k-points to describe the large supercell system (which could be the whole crystal). For our example of the 64-atom Si supercell, if there is no distortion of the diamond structure, the current reduced orbital method is the same as using one k-point of the 8-atom Si cubic cell to describe the 64-atom system. (By definition, using the $\bar{\Gamma}$ point of the 64-atom supercell to describe this 64-atom system is 'exact'.) Numerically, the density error of using one k-point of the 8-atom Si cubic cell to describe the Si crystal is found to be 4.5%, which is comparable to our charge density errors. In fact, this can be used as a way to estimate how many reduced orbitals (n) is needed to achieve an given accuracy. For a nonperiodic system, the reduced orbital method can be regarded as an extension of the k-point integration method. This is why at the end of section 1 we said that the current method is like a 'divide and conquer' method in k-space.

In the fixed-occ method, in order to use FFT to calculate $C(i, j, k)$ and $B(i, j, k)$ in Eqs (34) and (35), interpolation is used between the r-space grid and μ-space grid. This interpolation can introduce numerical errors, especially for gross grids. One way to implement the fixed-occ method is to calculate everything on the variable μ grid. Then the basis function is not the conventional plane wave, but $e^{ik\cdot\mu(r)}$. Application of the ∇_r^2 operator in equation (29) can be carried out in μ-space involving a transformation matrix for $r \to \mu(r)$. This approach is called the adaptive coordinate approach [23], and has been tested for various systems [24] to reduce the number of plane-wave functions. In this approach, the FFT can be directly used without interpolation in the calculation of $C(i, j, k)$ and $B(i, j, k)$.

In the fixed-vol method, the final step is very much like the method of Yang [9]. However, instead of making calculations for each small system with different bases, the current method first calculates $\{\phi_i(r)\}$ and uses this set as the basis for all the small systems. Because the calculation of $H_{i,j}(R)$ in equations (24) and (38) is easy, we can calculate for many R-points. Also, as the dimension n of $H_{i,j}(R)$ is only slightly larger than the number of occupied states in a small system, the diagonalization of $H_{i,j}(R)$ is very fast. The current weight function defined by equation (8), $w(r-R)$ used in equation (24) has small negative values in some regions. It is interesting to see whether using an always-positive weight function, like

$$w'(r) = \left((1/m) \sum_{2k \in \Omega} \exp(\mathrm{i}k \cdot r) \right)^2$$

in equation (24) will make any difference.

One 'bottleneck' of the current scheme is the solving of the linear equation (33). Using the current iterative method, it takes half the time of the whole calculation. However, if just a moderately accurate calculation is performed with a small number n of reduced orbitals, the orthonormal condition of equation (10) need not be satisfied exactly. In that case, we can minimize the following function:

$$F = E_{tot} + \gamma \sum_{i,j,k} \left| \int \phi_i(r)\phi_j^*(r) w_k(r)\, \mathrm{d}^3 r - \delta_{i,j}\delta_{k,0} \right|^2 \tag{42}$$

to calculate $\phi_i(r)$ without imposing any additional constraints on $\phi_i(r)$. Here, E_{tot} is defined in equation (13) and γ is an adjustable parameter. Again, the conjugate gradient method can be used to miminize F. For large γ, the second term of equation (42) at the minimum will be small, and equation (10) will be satisfied accurately. But for large γ, the convergence of the conjugate gradient iteration used to minimize F is slow due to the stiffness of the second term in equation (42). However, if equation (10) need only be satisfied approximately, we can use a smaller γ, and then the minimum of F can be found fairly easily. As a matter of fact, we found that, if the number n of reduced orbitals is small, a smaller γ can lead to a better charge density than an infinitely large γ. Using this approach, the problem of solving the linear equation (33) is avoided. Especially interesting is the use of this approach in the fixed-vol method; because in this method $\{\phi_i(r)\}$ serves only as a basis in the final diagonalization step (equation (24)), the accuracy (or, say, the convergence) of the $\phi_i(r)$, and whether they satisfy the exact orthogonalization conditions, would not be as critical as in the fixed-occ method (e.g., nonorthogonal basis diagonalization can be applied to $H_{i,j}(\boldsymbol{R})$ of equation (24)).

The advantage of the current method compared to the localized orbital method is that the plane-wave basis and the fast Fourier transformation technique can be readily used. Being an extension of the k-point integration method, the current method might work best for roughly uniform systems, like alloys or liquids. It remains to be seen how well the current method works for three-dimensional systems with surfaces and vacuums, where a dramatic variable-grid-$\mu(r)$ is needed in the fixed-occ method (although it works well for one-dimensional systems, as demonstrated in this work).

There is a problem in the localized orbital method analogous to our problems of equations (15) and (16) (with $w_k(r)$ defined in equation (11)) which leads us to introduce the variable grid $\mu(r)$ in the fixed-occ method. That is, we cannot put the allowed area of the localized orbitals uniformly in real space, disregarding the ionic positions in that region. Doing so will lead to a 'uniform' charge density which satisfies conditions like equation (15) (with $w_k(r)$ defined in equation (11)). Thus, the positions of the localized orbitals should accompany the positions of the ions, or let them float in a dynamical way. This is like our treatment of the variable grid $\mu(r)$. In fact, we can also determine $\mu(r)$ from ionic positions (instead of selfconsistently (dynamically) from $\rho(r)$), by assuming that the $\rho(r)$ and ionic charge follow each other (neutralized) in the scale of the small systems. This avoids the updating of $\mu(r)$ for each iteration step of $\phi_i(r)$ and makes equation (29) the true variational equation, and $\phi_i(r)$ the true variational solution for E_{tot} in equation (13).

The basic idea of the current work is that it is not necessary to use thousands of wholly spaced wavefunctions to describe the electronic structure of a very large system.

Thus, either we cut the space of each wavefunction and localize each wavefunction in a fixed finite region (the localized orbital method), or we cut the number of wholly spaced wavefunctions, using only a fixed number of them (the reduced orbital method). It turns out that we can work out the formulas for both approaches. It is the object of further studies to find the relationship between these two methods and to test the convergence of the current method with respect to the number of reduced orbitals n. It is of interest to see whether similar techniques, such as the unconstrained minimization approach reported in [13], could be used here. If this is possible, then the exact solution of linear equation (33) may become unnecessary. In our current procedure, for each conjugate gradient iteration on ϕ_i, we have ~ 30 conjugate gradient iterations on equation (33). Can we reduce this number and still get a converged result? Is this related to an unconstrained minimization scheme? We also need to study more carefully the speed of conjugate gradient convergence of $\phi_i(r)$ in this approach.

Acknowledgments

This work was done while L W Wang was at Cornell University and was partially reported in [8]. This work was partly supported by Corning Inc. The computational facilities for this work were provided in part by the Cornell–IBM Joint Study on Computing for Scientific Research.

References

[1] Hohenberg P and Kohn W M 1964 *Phys. Rev.* **136** 864
[2] Jones R O 1989 *Rev. Mod. Phys.* **61** 689
[3] Labonowski J K, Andzelm J W 1991 *Density Functional Methods in Chemistry* (New York: Springer)
[4] Kohn W and Sham L J 1965 *Phys. Rev.* A **140** 1133
[5] Ihm J, Zunger A and Cohen M L 1979 *J. Phys. C: Solid State Phys.* **12** 4409
[6] Car R and Parrinello M 1985 *Phys. Rev. Lett.* **55** 2471
[7] Teter M P, Payne M C and Allan D C, *Phys. Rev.* B **40** 2255
[8] Wang L W 1991 *PhD Thesis* Cornell University
Wang L W and Teter M P 1990 *Bull. Am. Phys. Soc.* **35** O9
[9] Yang W 1991 *Phys. Rev. Lett.* **66** 1438
[10] Wang L W and Teter M P 1992 *Phys. Rev.* B **45** 13 196
[11] Baroni S and Giannozzi P 1992 *Europhys. Lett.* **17** 547
[12] Galli G and Parrinello M 1992 *Phys. Rev. Lett.* **69** 3547
[13] Mauri F, Galli G and Car R 1993 *Phys. Rev.* B **47** 9973
Mauri F, Galli G, 1994 *Phys. Rev.* **B 50** 4316
[14] Wang L W and Teter M P 1992 *Phys. Rev.* B **46** 12 798
[15] Li X P, Nunes R W and Vanderbilt D 1993 *Phys. Rev.* B **47** 10 891
[16] Daw M S 1993 *Phys. Rev.* B **47** 10 895
[17] Ordejon P, Drabold D, Grumbach M and Martin R 1993 *Phys. Rev.* B **48** 14 646
[18] Kohn W 1993 *Chem. Phys. Lett.* **208** 167
[19] Drabold A D and Sankey O F 1993 *Phys. Rev. Lett.* **70** 3631
[20] Aoki M 1993 *Phys. Rev. Lett.* **71** 3842
[21] Kohn W 1959 *Phys. Rev.* **115** 809
Kohn W and Onffroy J R 1973 *Phys. Rev.* B **8** 2485
Cloizeaux J D 1964 *Phys. Rev.* **135** A698
[22] Payne M C, Teter M P, Allan D C, Arias T A and Joannopoulos J D 1992 *Rev. Mod. Phys.* **64** 1045
[23] Gygi F 1993 *Phys. Rev.* B **48** 11 692; 1992 *Europhys. Lett.* **19** 617
[24] Hamann D R unpublished